Flexible and Stretchable Brush-Painted Wearable Antenna on a 3D Printed Substrate

Muhammad Rizwan, *Student Member, IEEE*, M. Waqas A. Khan, *Student Member, IEEE*, Lauri Sydänheimo, *Member, IEEE*, Johanna Virkki, *Member, IEEE*, Leena Ukkonen, *Member, IEEE*.

Abstract— **This letter presents the proof-of-concept of the fabrication and performance analysis of a flexible and stretchable wearable antenna on a 3D printed substrate. It presents the details of the 3D printing of the substrate, brush-painting of the antenna, as well as the simulation and measurement results of the antenna. In addition, the bending test is done to check the limitation of the manufacturing method. The results show that the stretchable silver conductive paste achieves a 1.7×10^4 S/m conductivity. The fabricated antenna shows measured impedance bandwidth of 990 MHz (1.94 GHz – 2.93 GHz) with a peak gain of -7.2 dB at 2.45 GHz. Moreover, the antenna shows excellent wireless performance even when bent. Based on the results, the presented approach can be used for the manufacturing of wearable antennas and wireless on-body applications.**

Index Terms—**3D printing, brush-painting, NinjaFlex, on-body applications, wearable antenna.**

I. INTRODUCTION

3D printing has recently gained a lot of interest in several fields including the wireless electronics industry. This new printing technique allows the manufacturing of complex 3D models using layer by layer deposition of versatile materials [1-2]. This type of fabrication enables customized substrate structures (thickness, filling, shape), electrical properties (permittivity), and mechanical properties (weight, flexibility). The widely used materials for 3D printing are Acrylonitrile-Butadiene Styrene (ABS) and PolyLactic Acid (PLA). These materials have already been utilized in various antenna applications as substrates [3-5].

Currently, stretchable and flexible electronics are fundamentally changing the conception of electronics [6-7]. Due to the non-flexible and non-stretchable nature of ABS and PLA, they are not suitable candidates for such applications, including wearable applications, which enable devices integrated into clothes and affixed to skin. NinjaFlex is a new 3D printable material, composed of thermoplastic and rubber [8]. NinjaFlex is a strong, light weight, and flexible material, which makes it a good candidate for the fabrication of wearable Radio Frequency (RF) electronics and antennas [9-12]. Previously, the use of Fused Deposition Modeling (FDM) has been utilized to print NinjaFlex and the novel material has been successfully used as a substrate for wearable antennas [11-12]. In the previously reported work [11-12], copper tape has
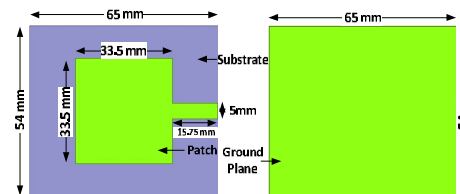

Fig. 1.　Antenna Dimensions (a) Patch (b) Ground.

been used as the conductive antenna material. However, the use of copper tape limits the flexibility and the reliability of the wearable antenna. Thus, there is a need for stretchable conductive material that can be effective deposited on the NinjaFlex substrate for use in wearable applications.

The aim of this paper is merely to develop a proof-of-concept of fabricating the flexible antenna on the 3D printed substrate by using stretchable silver conductive paste. This letter presents the fabrication of this novel antenna assembly and bending analysis of the fabricated antenna structure. To assess the wireless performance of this novel approach, both wireless measurements and electromagnetic field simulations are used.

II. ANTENNA DESIGN AND SIMULATION

A simple square patch antenna, presented in Fig. 1, is used to verify the novel fabrication method and material performance. ANSYS HFSS v.15 is used for antenna simulation and optimization. The antenna dimensions are optimized to resonate the antenna around 2.45 GHz and 2.5 GHz which cover the targeted industrial, scientific, and medical (ISM) band. The substrate is assigned properties of NinjaFlex, presented in [12]. The substrate height is set to 1.2 mm. A stretchable silver conductor paste (DuPont PE872 [13]) is used as the conductor. The measured conductivity of the paste is 1.7×10^4 S/m (conductivity measurement details are presented in Section IV) and it is assigned to the conductor in the simulation. Fig. 1 shows the final antenna, feed, and the substrate/ground plane dimensions. The ground plane, with the same dimensions as the substrate, is directly on the opposite side of the substrate.

Fig. 2 shows the simulation results of the antenna reflection coefficient in free space and near the human body. In the near human body simulation, the antenna is placed at a 5 mm distance from the body. The human body model presented in [14] is used with the properties of skin, fat, muscle, and bone at
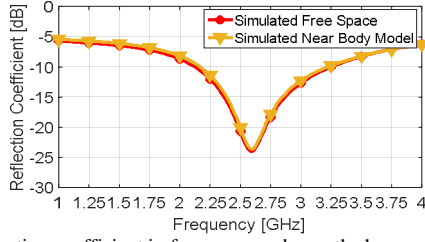
Fig. 2.   Reflection coefficient in free space and near the human body.

2.45 GHz. The antenna has -10 dB bandwidth of 1120 MHz (from 2.13 GHz to 3.25 GHz), which covers the targeted ISM band, as detailed in [14]. According to the simulation results, peak gain is -8.71 dB. The low gain can be explained by the relatively low conductivity of the stretchable silver conductor paste. The near body simulation results show a slight decrease in the reflection coefficient but the performance of the antenna stays robust. The main reason for this is the full ground plane of the antenna, which minimizes the effects of the human body. The simulated antenna directivity is 4.67 dB whereas its radiation efficiency is 2.81 %. In order to characterize the manufacturing method of the antenna presented in this work, the structure will be tested in air and not in a body-worn configuration.

III.   3D PRINTING OF THE SUBSTRATE MATERIAL

The printer used for this study is Prenta Duo 3D printer, which has two 1.75 mm nozzles for printing. The filament is installed on the side of the printer and it extends to the nozzles by using a plastic tube, as shown in Fig. 3.

To print the antenna substrate material (NinjaFlex), the printing speed is set to 35 mm/s with a nozzle printing temperature of 230-235 °C and a bed temperature of 60 °C. The substrate size is set to 65 mm x 54 mm x 1.2 mm (l×w×h) with each printing layer having the thickness of 0.2 mm and an infill of 100 %. Total of six layers are printed and a slicer tool is used for converting the substrate model to a 3D design. It takes approximately 45 minutes and 1955 mm filament to print the antenna substrate.

After printing the samples, the printed density is compared with filament density to determine the infill percentage. This results in a final infill of 83 %. The dielectric (2.8) and tangent loss (0.05) values in [12] are then used for all the simulations.
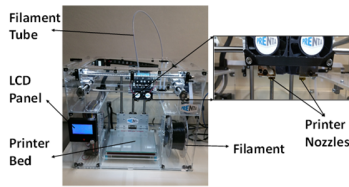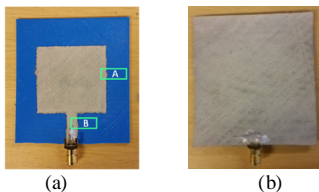

Fig. 3. Prenta 3D Printer.

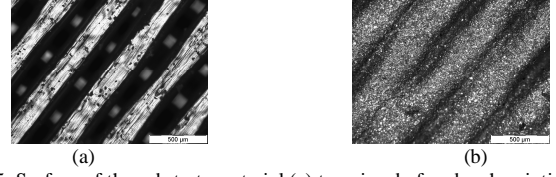| (a) | (b) |

Fig. 4. Fabricated antenna (a) patch (b) ground.

| (a) | (b) |

Fig. 5. Surface of the substrate material (a) top view before brush painting (b) top view after brush painting and thermal curing.

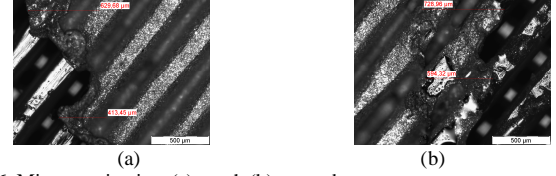| (a) | (b) |

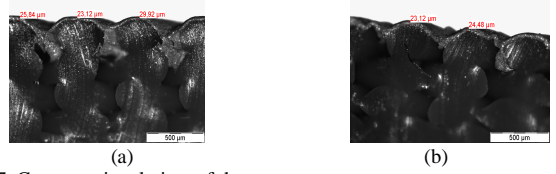Fig. 6. Microscopic view (a) patch (b) ground.

| (a) | (b) |

Fig. 7. Cross-sectional view of the antenna.

IV.   ANTENNA FABRICATION AND MEASUREMENT RESULTS

The fabrication of the antenna is done using brush-painting. The stretchable silver conductive paste is brush-painted on the NinjaFlex 3D printed substrate and the structure is thermally cured at 110 °C for 15 minutes (See Fig. 4 for the ready antenna assembly). The antenna patch and ground are separately brush-painted and cured one after the other. Fig. 5. shows the microscopic pictures (Olympus BX60M Microscope) of substrate's surface before and after the brush painting. The diagonal lines are visible because the substrate is printed using the rectilinear filling, as shown in Fig. 5(a). Fig. 5(b) clearly shows that the stretchable silver paste makes a continuous path and covers the surface well. Afterwards, a SubMiniature version A (SMA) connector is attached to the antenna with CircuitWorks conductive epoxy (CW2400) and the interconnection is cured at 70 °C for 10 minutes.

Fig. 6. shows a microscopic view of the patch and ground surfaces (part 'A' and 'B' from Fig. 4(a)). It can be seen that the edges of the patch and transmission line have some spreading of the conductive paste due to brush-painting. This can be considered as a fabrication inaccuracy. Fig. 7. shows the cross sectional view of the brush-painted antenna. The brush-painted silver conductive paste thickness has an average of 26.52 µm. Table I shows the measured sheet resistance and thickness, as well as the calculated resistivity and conductivity

TABLE I
FABRICATED SAMPLES PROPERTIES

Thickness [µm]	Sheet resistance [Ω/sq]	Resistivity [Ω.m]	Conductivity [S/m]
26.52	2.1	5.56×10^{-5}	1.7×10^{4}

TABLE II
EFFECT OF VARYING CONDUCTIVITY ON THE ANTENNA GAIN

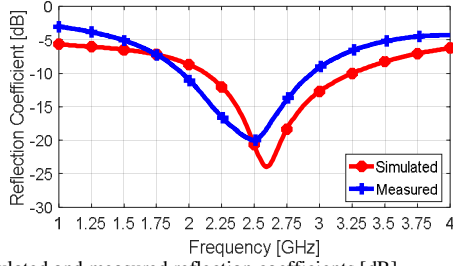| Analysis Type	Conductivity [S/m]	Gain [dB]
Simulation	1.6×10^{4}	- 9.14
	1.7×10^{4}	- 8.71
	3.0×10^{4}	- 5.79
Measurement	1.6×10^{4} S/m to 3.0×10^{4} S/m	- 7.20

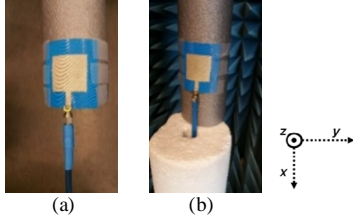Fig. 8. Simulated and measured reflection coefficients [dB].

Fig. 9. Bending test (a) top view (b) inside satimo star lab.

of the silver conductive paste.

The antenna reflection coefficient is measured with a Vector Network Analyzer (VNA) and the gain pattern is measured in Satimo Star lab. Fig. 8 shows the measured and simulated reflection coefficients, and that they are in good agreement. The minimum of the measured reflection coefficient occurs at 2.5 GHz and at 2.45 GHz it is -19.68 dB. The measured -10 dB bandwidth of the antenna is 990 MHz (from 1.94 GHz to 2.93 GHz). The measured peak gain of the antenna is -7.2 dB. The measured gain is 1.51 dB larger than the simulated, which can be explained by the conductivity of the silver layer. In the simulation, only fixed value of silver conductive paste (thickness of 25 µm and conductivity of 1.7×10^4 S/m) were used. However, the actual measured conductivity of the silver paste varies from 1.6×10^4 S/m to 3.0×10^4 S/m. Table II shows the effect of conductivity on the antenna gain. Three different values from the measured conductivity range (1.6×10^4 S/m to 3.0×10^4 S/m) are used to verify that the difference in the simulated and measured antenna gain is due to the varying conductivity. The measured -3 dB antenna beam width is approximately 37 degrees.

V. BENDING TEST

Next, a bending test is performed on the antenna structure in simulation as well as measurements. The bending test simulates the normal use environment of a wearable antenna, which can be placed on a body part where the surface is not flat. Also, bending can produce cracks in the conductor surface, or stretch it, which ultimately can affect the antenna performance.

To test the effects of bending, three cylindrical shaped polyethylene foams with radii 1.5 cm (small cylinder), 3.5 cm (medium cylinder) and 5.0 cm (large cylinder) are used. The bending angle is inversely proportional to the radius of the cylinder. The foam material of the cylinder does not affect the surface currents of the antenna. The antenna is bent on the cylinder in yz-plane as shown in Fig. 9. Transparent paper tape is used to hold the antenna in the proper positions during experiments. The same antenna is tested 4 times. However, the smaller bending (5 cm) is measured first, followed by 3.5 cm, and then 1.5 cm. Performance of the antenna is evaluated by

TABLE III
ANTENNA BENDING EFFECTS

Antenna Position	Reflection Coefficient at 2.45 GHz [dB]	Bandwidth [MHz]	Minimum Reflection Coefficient at [GHz]
Simulated (S) [Flat]	-18.28	1120 MHz (2.13 GHz – 3.25 GHz)	2.59
S Bending 1.5 cm	-12.15	480 MHz (2.10 GHz – 2.58 GHz)	2.32
S Bending 3.5 cm	-12.72	540 MHz (2.06 GHz – 2.60 GHz)	2.31
S Bending 5.5 cm	-16.98	650 MHz (2.11 GHz – 2.76 GHz)	2.41
Measured (M)[Flat]	-19.68	990 MHz (1.94 GHz – 2.93 GHz)	2.50
M Bending 1.5 cm	-18.57	960 MHz (1.96 GHz – 2.92 GHz)	2.33
M Bending 3.5 cm	-17.61	910 MHz (1.98 GHz – 2.89 GHz)	2.32
M Bending 5.0 cm	-19.15	970 MHz (1.96 GHz – 2.93 GHz)	2.40

analyzing the effects of bending on the reflection coefficient and radiation characteristics (radiation patterns at 2.45 GHz and efficiency on the selected frequency band).

Fig. 10 shows the variation in the reflection coefficient in flat and bend conditions (simulations and measurements). In general, bending the antenna changes the effective length, which ultimately changes the resonant frequency [15]. In both simulation and measurements, it can be seen that the change in the effective length shifts the frequency slightly to a lower value. However, the antenna operates at 2.45 GHz in all the cases. After bending measurements; no cracks are observed, under a microscope, on the surface of the antenna and the performance returned to normal after bending. Table III summarizes the effect of bending on the reflection coefficient and the -10 dB bandwidth of the antenna. From Fig. 10 and Table III (frequency of minimum reflection coefficient) it can be clearly seen that the frequency shift after the bending in simulation and measurements stays the same.

Fig. 11 shows the 2D yz-plane simulated and measured radiation pattern of the antenna in the studied cases of the bending at 2.45 GHz. The radiation patterns and the efficiencies
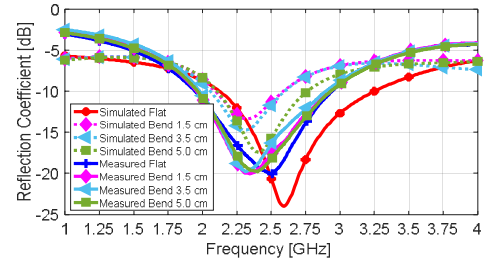

Fig. 10. Effect of bending on the reflection coefficient [dB] of the antenna.
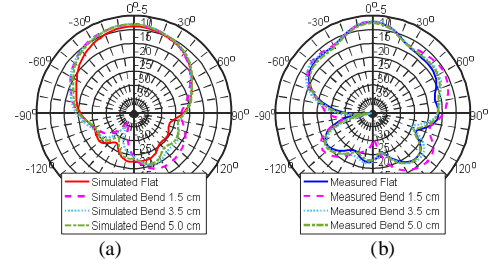

Fig. 11. Effect of bending on the 2D radiation pattern of the antenna (a) Simulated (b) Measured.
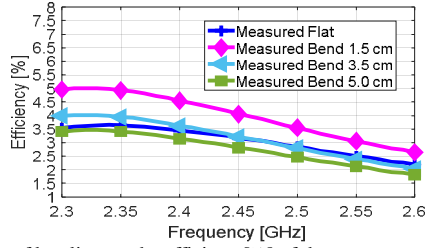
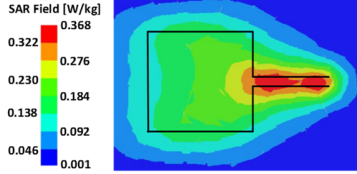Fig. 12. Effect of bending on the efficieny [%] of the antenna.

Fig. 13. Local SAR distribution on the skin at 2.45 GHz.

are measured using Satimo Star Lab. A slight increase in the beam width is observed when the antenna is placed on the large cylinder. The increase in the beam width becomes more prominent when the antenna is placed on the small cylinder. The increase in the beam width decreases the directivity of the antenna. Fig. 12 shows the effect of bending on the total efficiency of the antenna, which takes into account both matching and radiation efficiencies, and is measured by Satimo Star Lab equipment. It can be seen that the efficiency stays the same for small bending but for larger bending there is a slight increase. As the peak gain of the antenna stays same (see Fig. 11), and the directivity decreases with increasing bending, the total efficiency increases. The slight decrease in efficiency in the 5 cm bending case is because the matching is also decreased when compared to the measured flat antenna. The simulation and measurement results are in good matching. Overall, the fabricated antenna performance has shown to be robust to structural deformation like bending. Another important consideration is the low efficiency of the antenna. However, better wireless properties with the same substrate material and stretchable silver paste can be achieved by 3D dispensing the antenna [16].

VI. SAR CALCULATIONS AND NEAR BODY SIMULATION

The skin is the closest tissue to the wearable antenna and, as a result, the maximum Specific Absorption Rate (SAR) occurs in the skin. The maximum amount of power radiated from the antenna is limited by the SAR. We have followed the U.S. Federal Communications Commission (FCC) regulation: $SAR_{max} = 1.6$ W/kg and estimated the SAR in a model where a skin block of $18.75 \times 18.75 \times 30$ cm^3 is located at a 5 mm distance from the antenna, by using the details in [17]. Power of 1 W is supplied to the antenna to evaluate the SAR performance that resulted in a SAR value of 0.368 W/kg. This is well below the SAR_{max} limit of 1.6 W/kg. Fig. 13 shows the local SAR distribution on the skin at 2.45 GHz. It can be clearly seen that the fabricated antenna follows the FCC regulations.

VII. CONCLUSION

This letter presents the proof-of-concept of the fabrication and performance analysis of a flexible and stretchable wearable antenna on a 3D printed substrate. The substrate is 3D printed using NinjaFlex material and the patch antenna is brush-painted from stretchable silver conductive paste. To demonstrate the potential of the manufacturing approach, the wireless performance of the fabricated antenna is analyzed in initial (flat) and in different bending positions. The results show that the antenna operates well in all considered scenarios with a good impedance matching and efficiency. According to SAR simulations, the fabricated antenna can be used near the skin in future wearable applications. Based on our results, these novel fabrication methods and materials can be used for integration of antennas on versatile flexible structures. Future work includes humidity tests and studies about potential protective coatings to improve the reliability of the antenna in harsh environments.

REFERENCES

[1] I. Gibson, D. W. Rosen, and B. Stucker, Additive Manufacturing Technologies: Rapid Prototyping to Direct Digital Manufacturing, New York: Springer, 2010.

[2] H. Lipson and M. Kurman, Fabricated: The New World of 3D Printing, Wiley, USA, 2013.

[3] M. Mirzaee and S. Noghanian, "Additive manufacturing of a compact 3D dipole antenna using ABS thermoplastic and high temperature carbon paste," *IEEE International Symposium on Antennas and Propagation* (APSURSI), pp. 475-476, Jun., 2016.

[4] M. Hoyack et al., "Connector design for 3D printed antennas," *IEEE International Symposium on Antennas and Propagation* (APSURSI), pp. 477-478, Jun., 2016.

[5] M. Mirzaee, S. Noghanian, L. Wiest and I. Chang, "Developing flexible 3D printed antenna using conductive ABS materials," *IEEE International Symposium on Antennas and Propagation & USNC/URSI National Radio Science Meeting*, pp. 1308-1309, Jul., 2015.

[6] J. A. Rogers, T. Someya, Y. G. Huang "Materials and mechanics for stretchable electronics," *Science*, vol. 327, no. 5973, pp. 1603-1607, Mar., 2010.

[7] J. A. Fan et al., "Fractal design concepts for stretchable electronics," *Nat. Commun.*, vol. 5, no. 3266, Feb., 2014.

[8] https://ninjatek.com/[site accessed on 22nd Nov 2016]

[9] R. Bahr et al., "RF characterization of 3D printed flexible materials - NinjaFlex Filaments," *European Microwave Conference (EuMC)*, pp. 742-745, Sept., 2015.

[10] E. Massoni et al., "Characterization of 3D-printed dielectric substrates with different infill for microwave applications," *IEEE MTT-S International Microwave Workshop Series on Advanced Materials and Processes for RF and THz Applications (IMWS-AMP)*, pp. 1-4, Jul., 2016.

[11] K. Nate and M. M. Tentzeris, "A novel 3-D printed loop antenna using flexible NinjaFlex material for wearable and IoT applications," *IEEE Electrical Performance of Electronic Packaging and Systems (EPEPS)*, pp. 171-174, Oct., 2015,.

[12] S. Moscato et al., "Infill-Dependent 3-D-Printed Material Based on NinjaFlex Filament for Antenna Applications," *IEEE Antennas and Wireless Propagation Letters*, vol. 15, no. pp. 1506-1509, Jan., 2016.

[13] http://www.dupont.com/ [site accessed on 22nd Nov 2016].

[14] M. Rizwan et al., "Performance evaluation of circularly polarized patch antenna on flexible EPDM substrate near human body," Loughborough Antennas & Propagation Conference (LAPC), pp. 1-5, Jan., 2015.

[15] M. Rizwan et al., "Impact of Bending on the Performance of Circularly Polarized Wearable Antenna", *PIERS Proceedings*, pp. 732-737, Aug., 2015.

[16] M. Rizwan, M. W. A. Khan, H. He, J. Virkki, L. Sydänheimo and L. Ukkonen, "Flexible and stretchable 3D printed passive UHF RFID tag," IET Electronics Letters, vol. 53, no. 15, pp. 1054-1056, Jul 2017.

[17] M. W. A. Khan et al., "Characterization of Two-Turns External Loop Antenna With Magnetic Core for Efficient Wireless Powering of Cortical Implants," *IEEE Antennas and Wireless Propagation Letters*, vol. 15, pp. 1410-1413, Dec., 2016.